NORS/NDACC/GAW workshop
Brussels, 5-7 November, 2014

Have we missed an early stratospheric warning signal for the greenhouse effect?

C. S. Zerefos*, K. Tourpali, P. Zanis, K. Eleftheratos, C. Repapis, A. Goodman, D. Wuebbles, I.S.A. Isaksen and J. Luterbacher

* zerefos@geol.uoa.gr

Sulfur Emissions

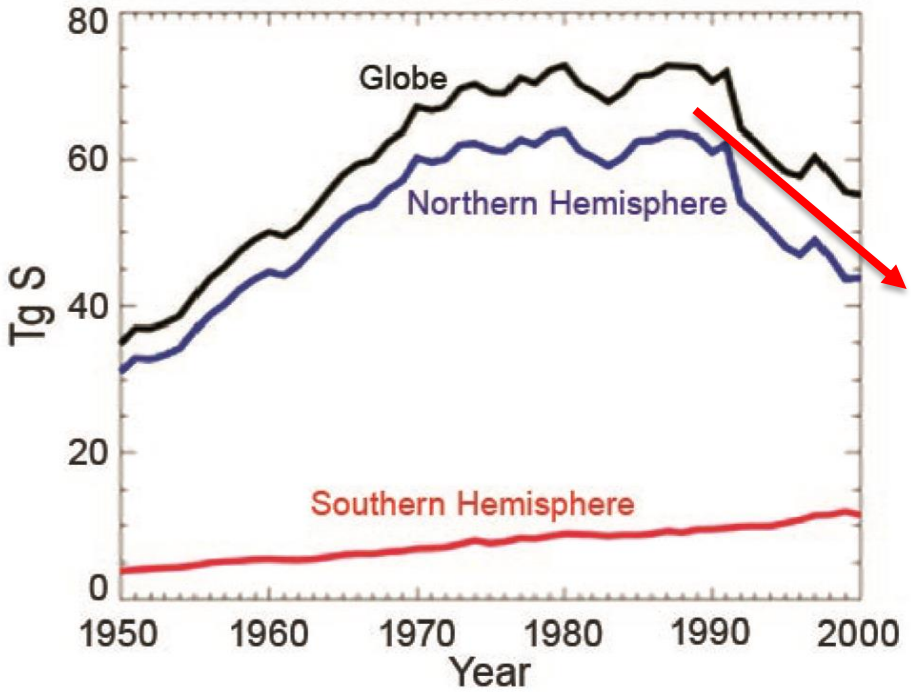

~ 1.5 Tg S yr^{-1}

Annual sulfur emission estimates from 1950–2000 over the NH (blue line), the SH (red line), and the entire globe (black line) according to (Stern 2006). Units are teragrams of sulfur (Tg S).

Wild, 2012

Observed tendencies in surface solar radiation

	1950s-1980s	1980s-2000	after 2000
USA	-6	5	8
Europe	-3	2	3
Japan	-5	8	0
China/Mongolia	-7	3	-4
India	-3	-8	-10

Changes in surface solar radiation observed in regions with good station coverage during three periods. (left column) The 1950s–1980s show predominant declines ("dimming"), (middle column) the 1980s–2000 indicate partial recoveries ("brightening") at many locations, except India, and (right column) recent developments after 2000 show mixed tendencies. Numbers denote typical literature estimates for the specified region and period in W m^{-2} per decade. Based on various sources as referenced in Wild (2009).

Wild, 2012

Impact on global warming

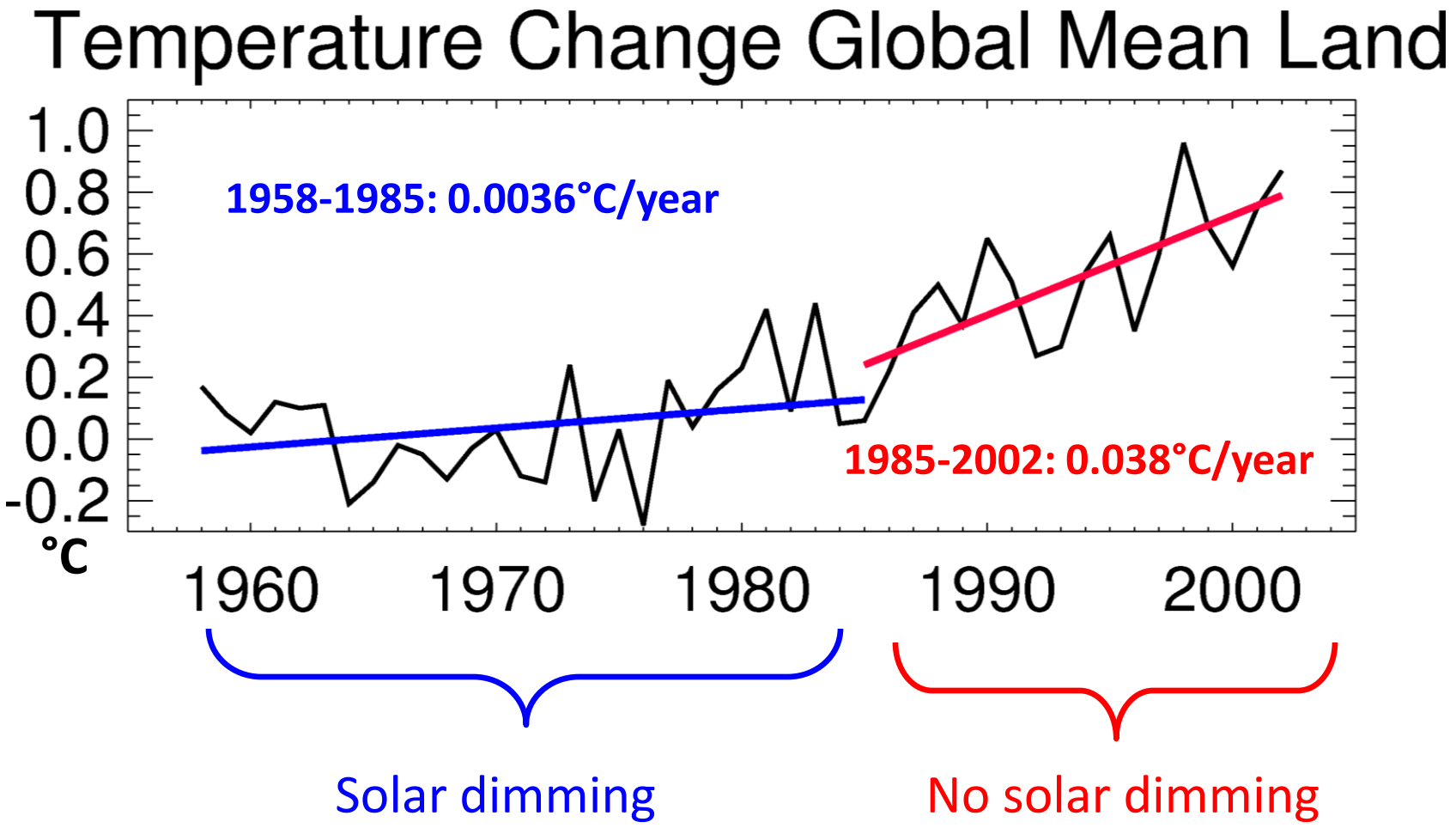

Wild et al. 2007 GRL 34

from Wild, 2008

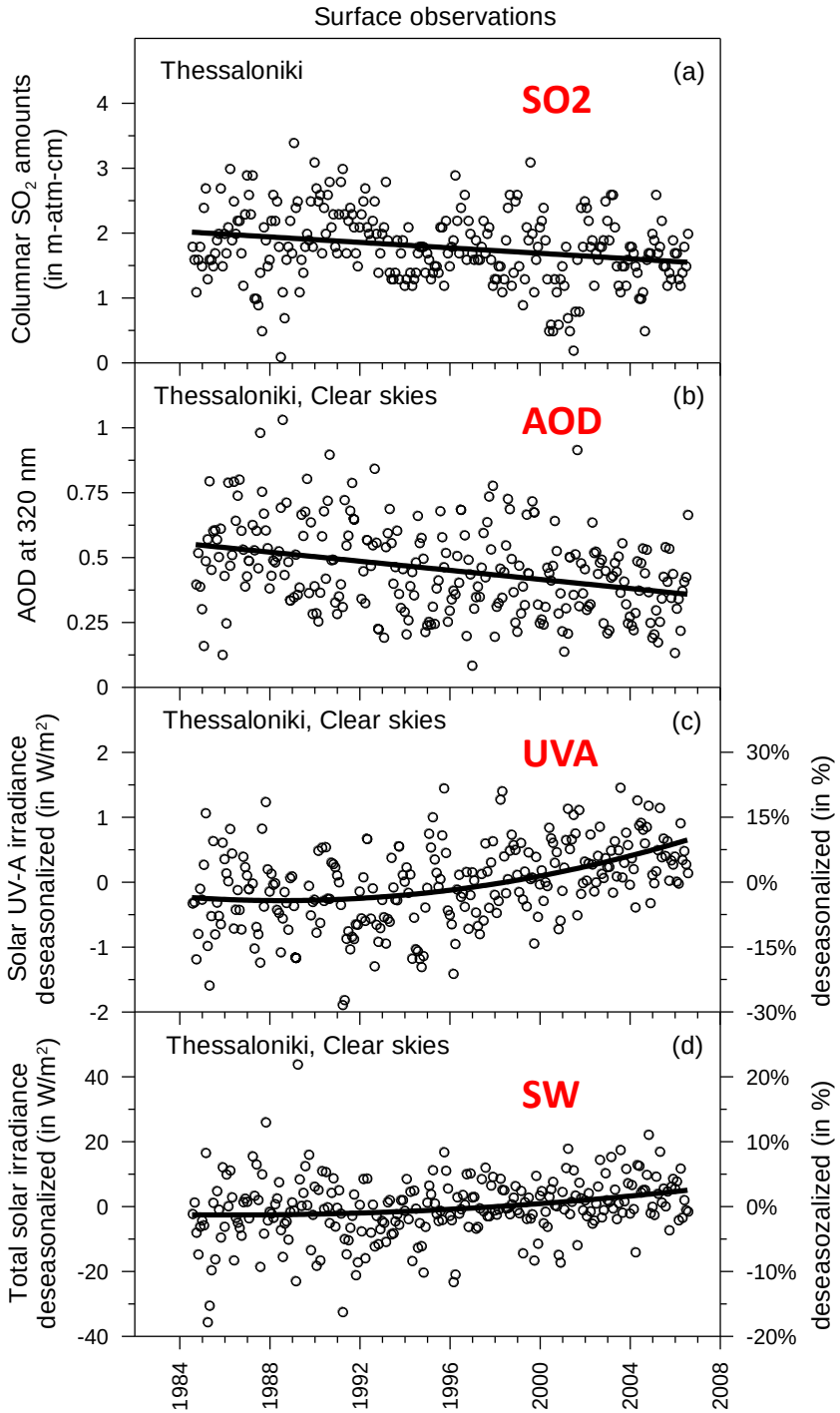

Both the negative rate of change (dimming) and the positive rate of change (brightening) are amplified in the UV-A solar irradiances in comparison to the total solar irradiance by a factor of 2.6

(a) Mean monthly SO2 over Thessaloniki.
(b) Mean monthly AOD at 320 nm.
(c) Deseasonalized solar UV-A irradiances.
(d) Deseasonalized total solar irradiance.

Zerefos et al., 2009, Tellus-B

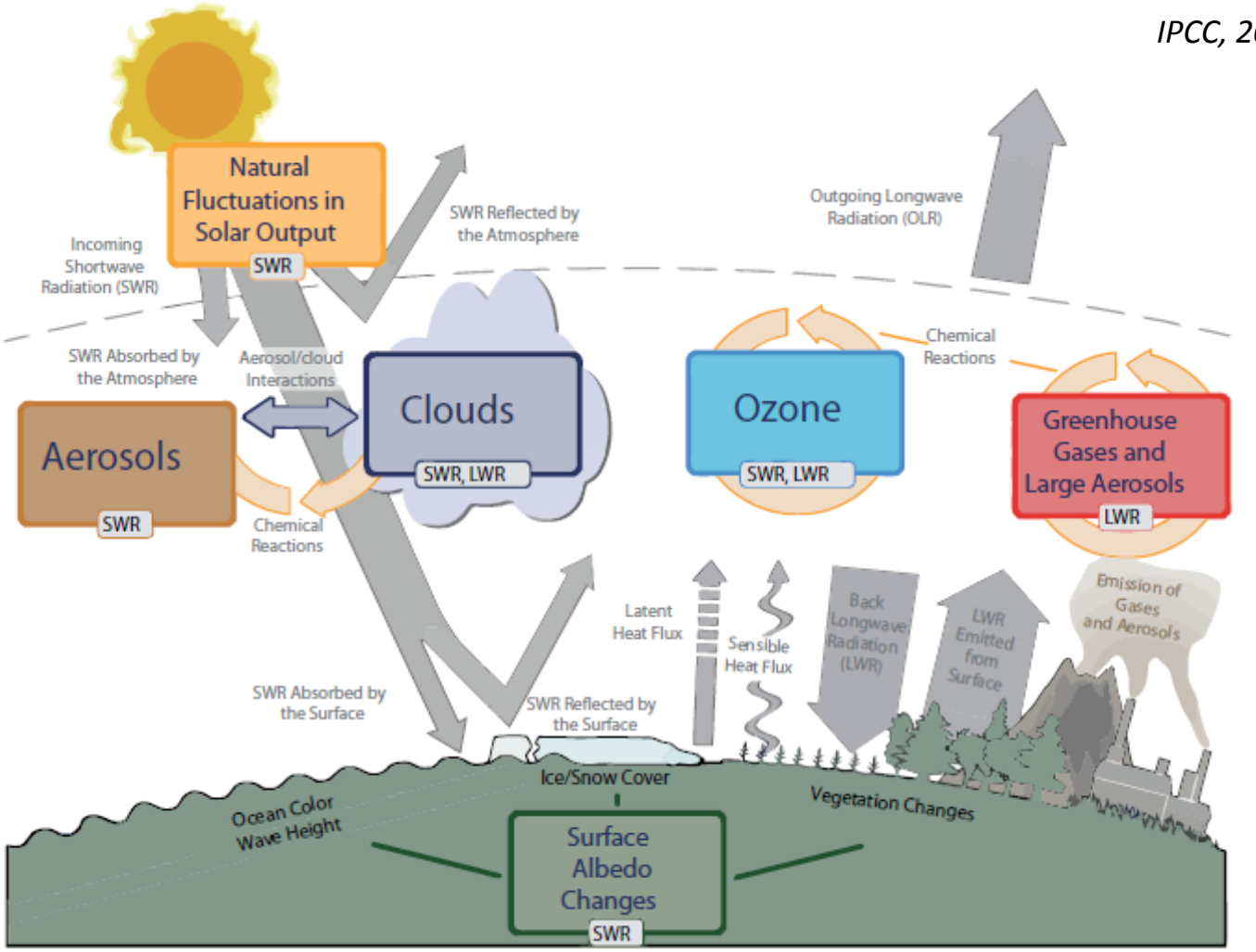

Figure 1.1 | Main drivers of climate change. The radiative balance between incoming solar shortwave radiation (SWR) and outgoing longwave radiation (OLR) is influenced by global climate 'drivers'. Natural fluctuations in solar output (solar cycles) can cause changes in the energy balance (through fluctuations in the amount of incoming SWR). Human activity changes the emissions of gases and aerosols, which are involved in atmospheric chemical reactions, resulting in modified O3 and aerosol amounts. O3 and aerosol particles absorb, scatter and reflect SWR, changing the energy balance. Some aerosols act as cloud condensation nuclei modifying the properties of cloud droplets and possibly affecting precipitation. Because cloud interactions with SWR and LWR are large, small changes in the properties of clouds have important implications for the radiative budget. Anthropogenic changes in GHGs (e.g., CO2, CH4, N2O, O3, CFCs) and large aerosols (>2.5 µm in size) modify the amount of outgoing LWR by absorbing outgoing LWR and re-emitting less energy at a lower temperature. Surface albedo is changed by changes in vegetation or land surface properties, snow or ice cover and ocean colour (Section 2.3). These changes are driven by natural seasonal and diurnal changes (e.g., snow cover), as well as human influence (e.g., changes in vegetation types) (Forster et al., 2007).

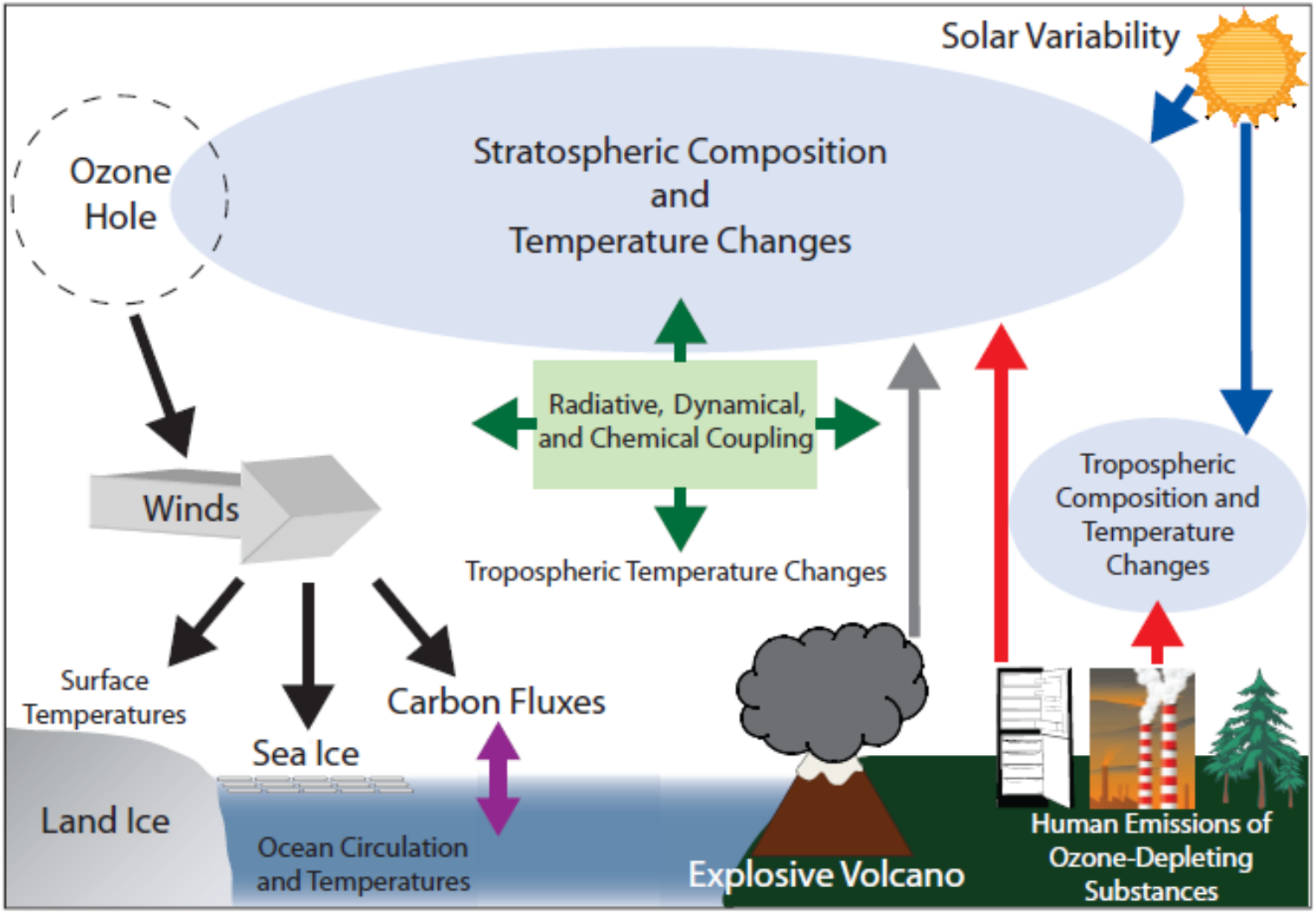

Schematic of the drivers and mechanisms considered for stratospheric changes and climate

Ozone Assessment, 2010, Chapter 4

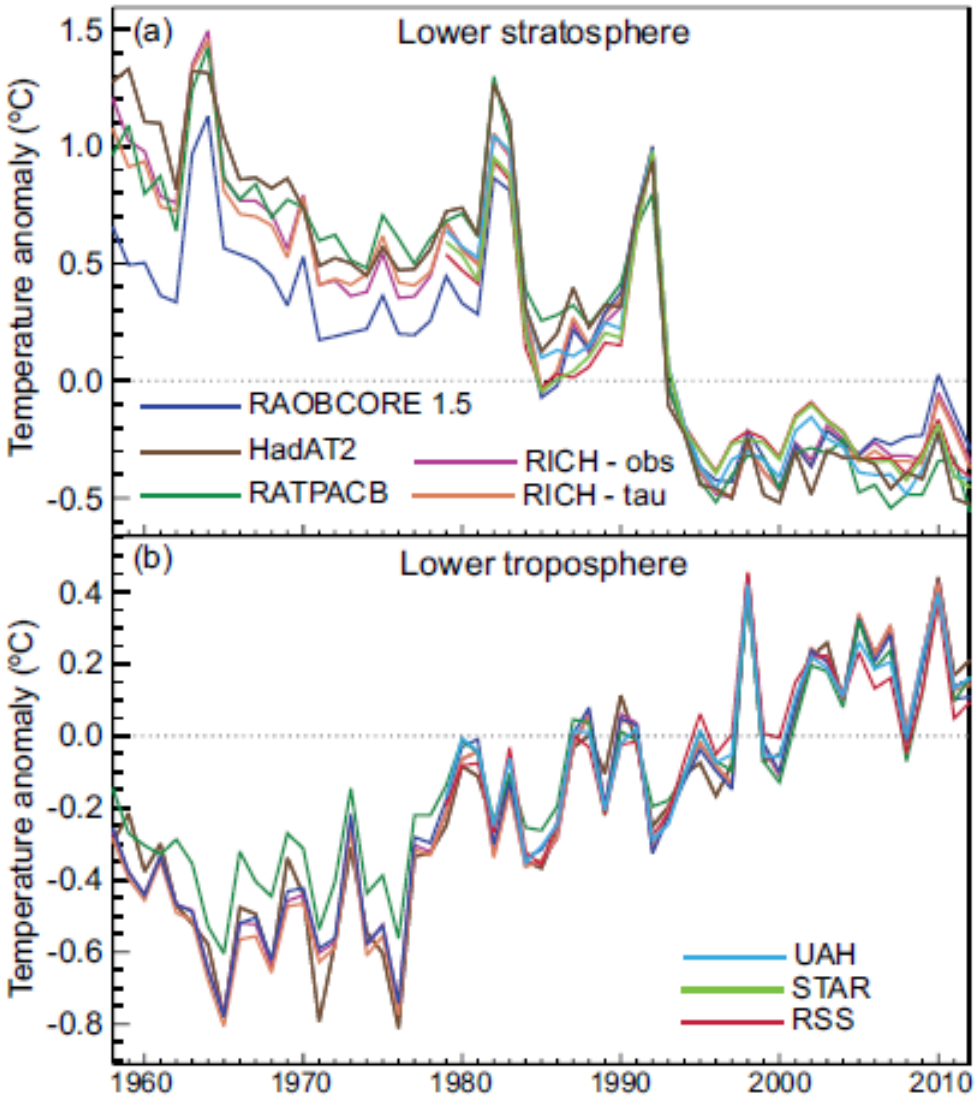

Figure 2.24 | Global annual average lower stratospheric (top) and lower tropospheric (bottom) temperature anomalies relative to a 1981–2010 climatology from different data sets. STAR does not produce a lower tropospheric temperature product. Note that the y-axis resolution differs between the two panels.

IPCC, 2013, Chapter 2

Objectives

A major open question that still remains to be answered is if the stratosphere can be considered as a more suitable region than the troposphere to detect anthropogenic climate change signals and what can be learned from the long-term stratospheric temperature trends. Indeed the signal-to-noise ratio in the stratosphere is, radiatively speaking, more sensitive to anthropogenic GHGs forcing and less disturbed from natural variability of water vapour and clouds when compared to the troposphere. This is because (a) the dependence of the equilibrium temperature of the stratosphere on CO_2 is larger than that on tropospheric temperature, (b) the equilibrium temperature of the stratosphere depends less upon tropospheric water vapour variability and (c) the influence of cloudiness upon equilibrium temperature is more pronounced in the troposphere than in the stratosphere where the influence decreases with height (Manabe and Weatherald, 1967). Furthermore, anthropogenic aerosols are mainly spread within the lower troposphere (He et al., 2008), and presumably have little effect on stratospheric temperatures.

Zerefos et al., ACP, 2014

Objectives (cont'd)

Another open question is if the lower stratosphere started cooling since the time a reasonable global network became available i.e. after the International Geophysical Year (IGY) in 1957-1958. Such a long lasting cooling from the 60s until today needs to be re-examined and explained. To what extent are the cooling trends in the lower stratosphere related to human induced climate change? Has it been accelerating, for instance at high latitudes in winter/spring due to ozone depletion? Has it been interrupted by major volcanic eruptions and El Nino events (Zerefos et al., 1992) or large climatological anomalies?

The study addresses those questions and presents a new look at observed temperature trends over the Northern Hemisphere from the troposphere up to the lower stratosphere in a search for an early warning signal of global warming i.e. a cooling in the lower stratosphere relative to the warming in the lower atmosphere.

Zerefos et al., ACP, 2014

Data sources

Tropospheric and stratospheric temperature, pressure and geopotential height data used in this study are based on the following sources:

a) the NCEP/NCAR reanalysis I product (NCEP) data from 1958 to 2011 (Kalnay et al., 1996; Kistler et al., 2001),
b) the Free University of Berlin (FU-Berlin) from 1958 to 2001,
c) the Radiosonde Innovation Composite Homogenization (RICH) data (Haimberger, 2007; Haimberger et al., 2008) from 1958 to 2006 and
d) historical simulations with the NCAR Community Earth System Model (CESM) coupled to the "high-top" Whole Atmosphere Community Climate Model (WACCM) CESM1-WACCM (Marsh et al., 2013) from 1958 to 2005.

Our analysis is focused at the northern hemisphere, as the data coverage in the pre-satellite era has been denser there than at the southern hemisphere.

Zerefos et al., ACP, 2014

Figure 1: Layer mean temperature variations in northern hemisphere summer (JJA) at layers 925-500 hPa, 500-300 hPa, 100-50 hPa and 50-30 hPa calculated from NCEP reanalysis and FU-Berlin datasets and filtered from natural variations for three latitudinal belts a) 5N-30N, b) 30N - 60N and c) 60N - 90N.

The respective summer normalised time series of temperature from RICH dataset at levels 850 hPa, 500 hPa, 50 hPa and 30 hPa are also illustrated as well as the NCEP tropopause pressure.

The trends lines before and after 1979 are superimposed. Grey lines denote NCEP reanalysis variations. Green lines denote variations as depicted in the FU-Berlin analysis, while purple dotted lines the RICH data temperature. The units at vertical axis are in degrees ^{o}C except for the tropopause that is in hPa.

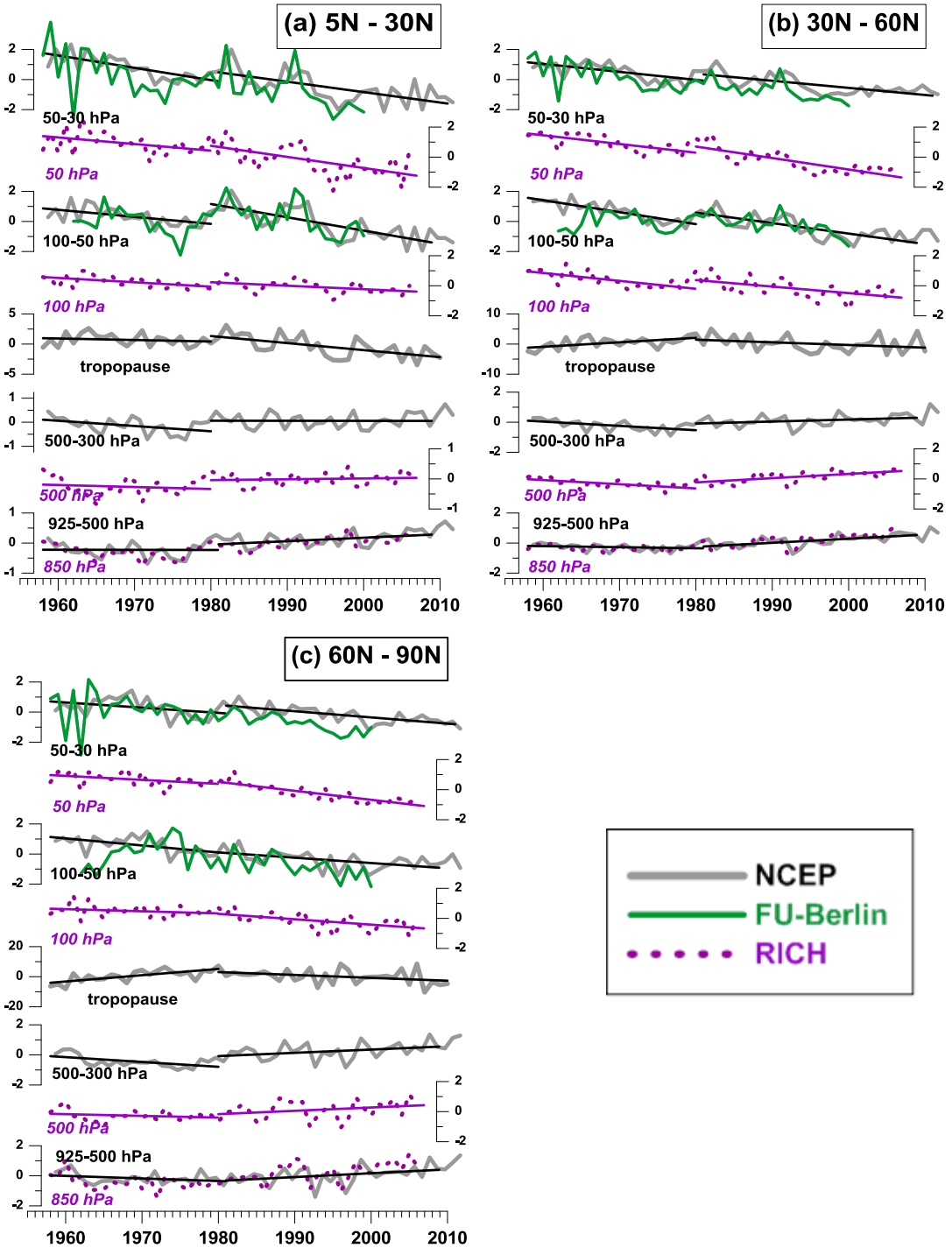

Table 1: Trend calculations in northern hemisphere summer (JJA) based on the monthly normalised time series of the layer mean temperature (°C/decade) and tropopause pressure (hPa/decade) calculated from NCEP reanalysis and filtered from natural variations at the latitudinal belts a) 5 N-30 N, b) 30 N - 60 N and c) 60 N - 90 N.

The layers are:
L1: 1000-925 hPa, L2: 925-500 hPa, L3: 500-300 hPa, L4: 100-50 hPa and L5: 50-30 hPa.

The trends calculations refer to the periods 1958-1979, 1980-2001, 1980-2005 and 1980-2011.

Layer	90–60° N Trend	90–60° N *t* test	60–30° N Trend	60–30° N *t* test	30–05° N Trend	30–05° N *t* test
Period 1958–1979						
L1	0.26 ± 0.11	2.48	-0.01 ± 0.04	−0.25	0.11 ± 0.03	3.91
L2	0.10 ± 0.09	1.12	-0.11 ± 0.04	−2.92	-0.01 ± 0.04	−0.22
L3	-0.42 ± 0.07	−5.69	-0.25 ± 0.04	−6.89	-0.11 ± 0.05	−2.19
L4	-0.57 ± 0.31	−1.83	-0.59 ± 0.06	−10.37	-0.21 ± 0.12	−1.79
L5	-0.77 ± 0.35	−2.19	-0.74 ± 0.09	−8.38	-0.59 ± 0.10	−5.99
TP	1.98 ± 1.25	1.58	2.42 ± 0.28	8.57	0.19 ± 0.24	0.78
Period 1980–2001						
L1	0.39 ± 0.11	3.42	0.23 ± 0.04	5.31	0.06 ± 0.03	2.00
L2	0.05 ± 0.09	0.56	0.19 ± 0.04	4.74	0.04 ± 0.04	0.93
L3	0.14 ± 0.08	1.83	0.07 ± 0.04	1.50	-0.10 ± 0.05	−2.20
L4	-0.70 ± 0.34	−2.04	-0.94 ± 0.07	−14.14	-0.90 ± 0.11	−8.30
L5	-0.66 ± 0.36	−1.84	-0.83 ± 0.08	−10.02	-0.73 ± 0.09	−8.20
TP	-1.87 ± 1.69	−1.10	-1.59 ± 0.35	−4.52	-0.82 ± 0.24	−3.43
Period 1980–2005						
L1	0.61 ± 0.09	6.75	0.28 ± 0.03	8.31	0.11 ± 0.02	5.51
L2	0.14 ± 0.07	2.07	0.24 ± 0.03	7.81	0.11 ± 0.03	3.67
L3	0.23 ± 0.06	3.91	0.11 ± 0.03	3.20	-0.01 ± 0.03	−0.35
L4	-0.43 ± 0.26	−1.61	-0.69 ± 0.06	−11.86	-0.79 ± 0.08	−9.51
L5	-0.46 ± 0.28	−1.66	-0.63 ± 0.07	−9.14	-0.55 ± 0.08	−6.90
TP	-1.06 ± 1.30	−0.82	-0.72 ± 0.27	−2.68	-0.75 ± 0.18	−4.14
Period 1980–2011						
L1	0.65 ± 0.07	9.18	0.29 ± 0.03	10.83	0.13 ± 0.02	7.85
L2	0.25 ± 0.05	4.68	0.27 ± 0.03	10.50	0.16 ± 0.02	6.40
L3	0.28 ± 0.05	5.99	0.16 ± 0.03	5.91	0.07 ± 0.03	2.22
L4	-0.32 ± 0.22	−1.50	-0.53 ± 0.05	−10.03	-0.67 ± 0.07	−10.21
L5	-0.38 ± 0.22	−1.70	-0.45 ± 0.06	−7.59	-0.41 ± 0.06	−6.51
TP	-1.49 ± 1.07	−1.40	-1.07 ± 0.25	−4.23	-0.91 ± 0.15	−5.92

Figure 2: Monthly normalised time series of the layer mean temperature at layers 925-500 hPa, 500-300 hPa, 100-50 hPa and 50-30 hPa calculated from NCEP reanalysis and FU-Berlin datasets for the northern hemisphere and filtered from natural variations at the latitudinal belts a) 5 N-30 N, b) 30 N - 60 N and c) 60 N - 90 N.

The respective monthly normalised time series of temperature from RICH dataset at levels 850 hPa, 500 hPa, 50 hPa and 30 hPa are also illustrated with purple lines as well as the NCEP tropopause pressure normalized monthly means.

The trends lines before and after 1979 are also superimposed. The units at vertical axis are in degrees ^{o}C except for the tropopause that is in hPa.

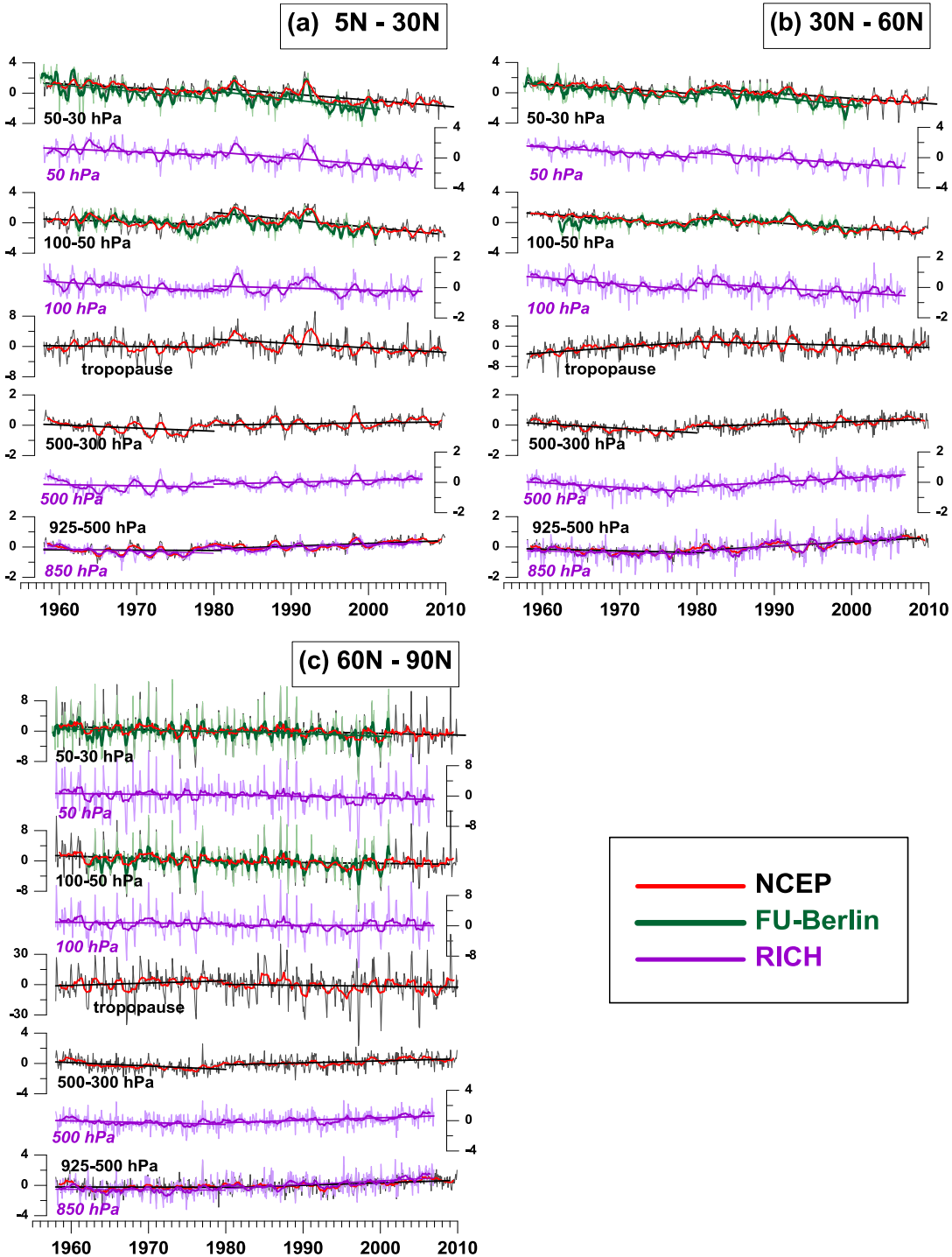

Figure 3: Layer mean temperature trends (°C/decade) for each month (x-axis) and layer (y-axis) based on NCEP reanalysis over the periods 1958-1979 and 1980-2005, respectively, for three latitudinal belts a) and b) for 5N-30N, c) and d) for 30N - 60N and e) and f) for 60N - 90N.

The layers are: Layer 1: 1000-925 hPa, Layer 2: 925-500 hPa, Layer 3: 500-300 hPa, Layer 4: 100-50 hPa, Layer 5: 50-30 hPa, and Layer 6: 30-10 hPa.

The shaded areas are non-statistically significant at 90% confidence level.

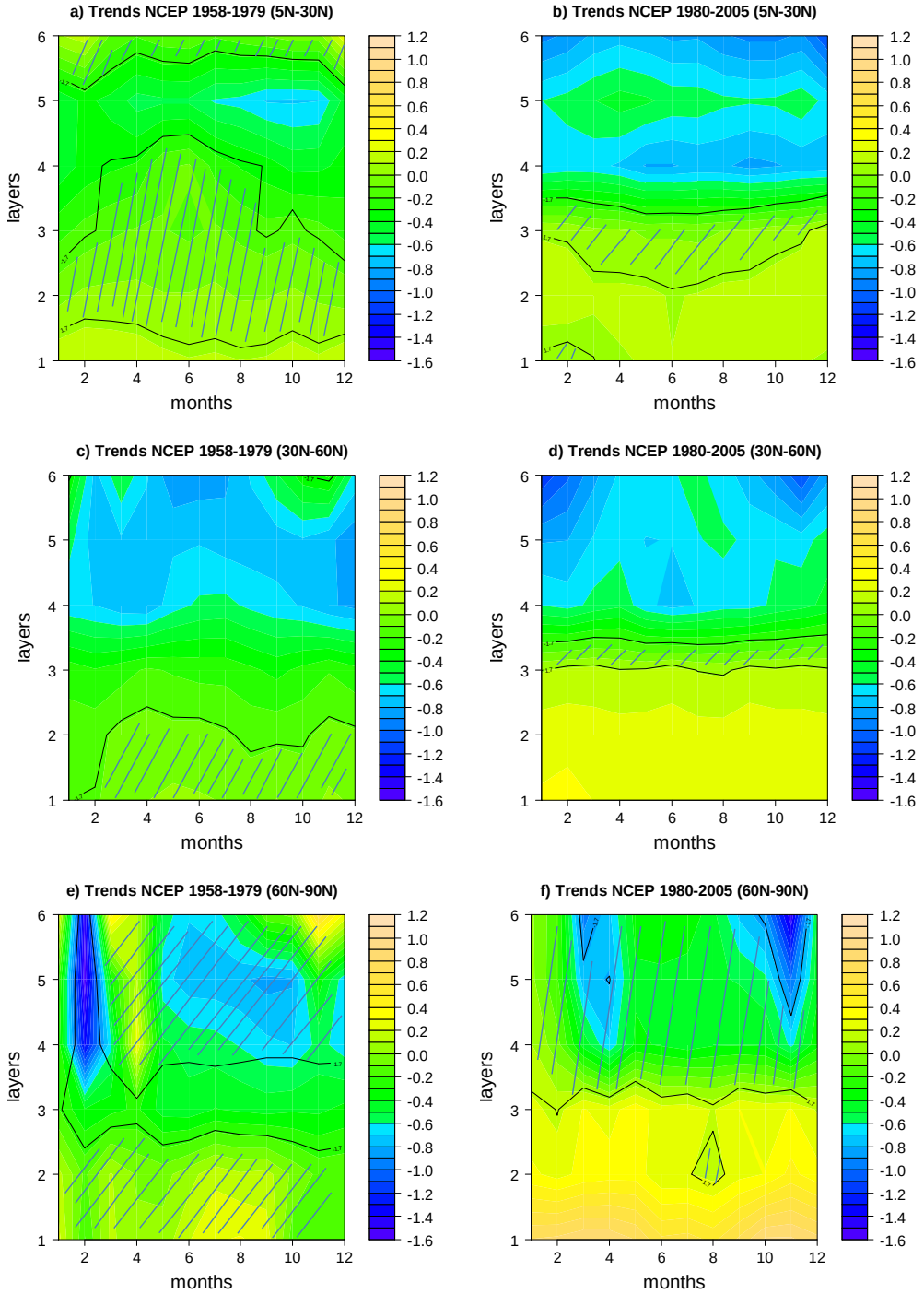

Figure 4: Temperature trends (°C/decade) for each month (x-axis) and level (y-axis) based on RICH dataset over the periods 1958-1979 and 1980-2005, respectively, for three latitudinal belts a) and b) for 5N-30N, c) and d) for 30N - 60N and e) and f) for 60N - 90N.

The levels are: Level 1: 850 hPa, Level 2: 500 hPa, Level 3: 300 hPa, Level 4: 100 hPa, Level 5: 50 hPa, and Level 6: 30 hPa.

The shaded areas are non-statistically significant at 90% confidence level.

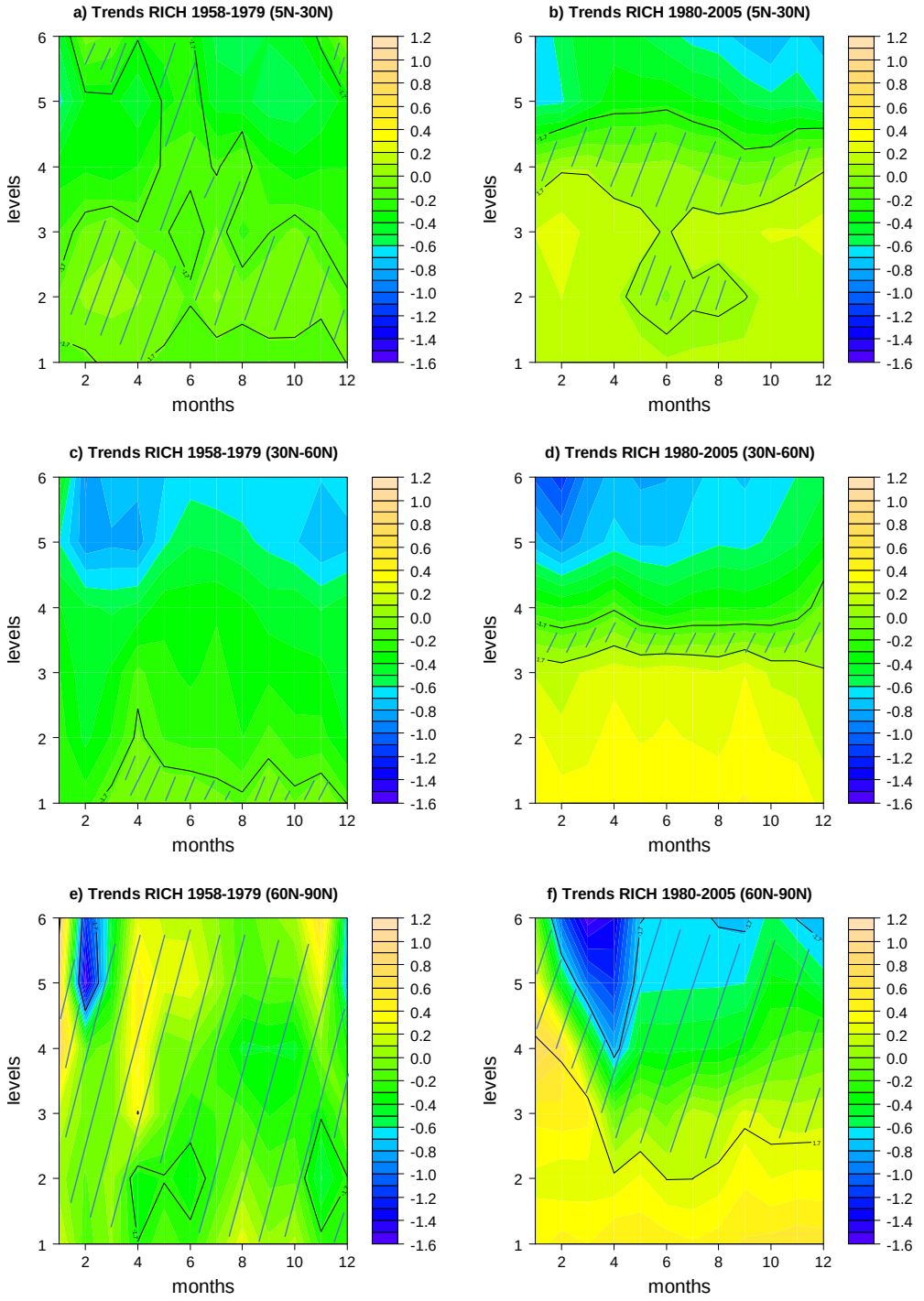

Figure 5: Mean temperature trends (°C/decade) for each month (x-axis) based on FU-Berlin dataset over the periods 1958-1979 and 1980-2001 for the layers 100-50 hPa (a and b) and 50-30 hPa (c and d) for the three latitudinal belts, 5N-30N (blue), 30N - 60N (green) and 60N - 90N (red).

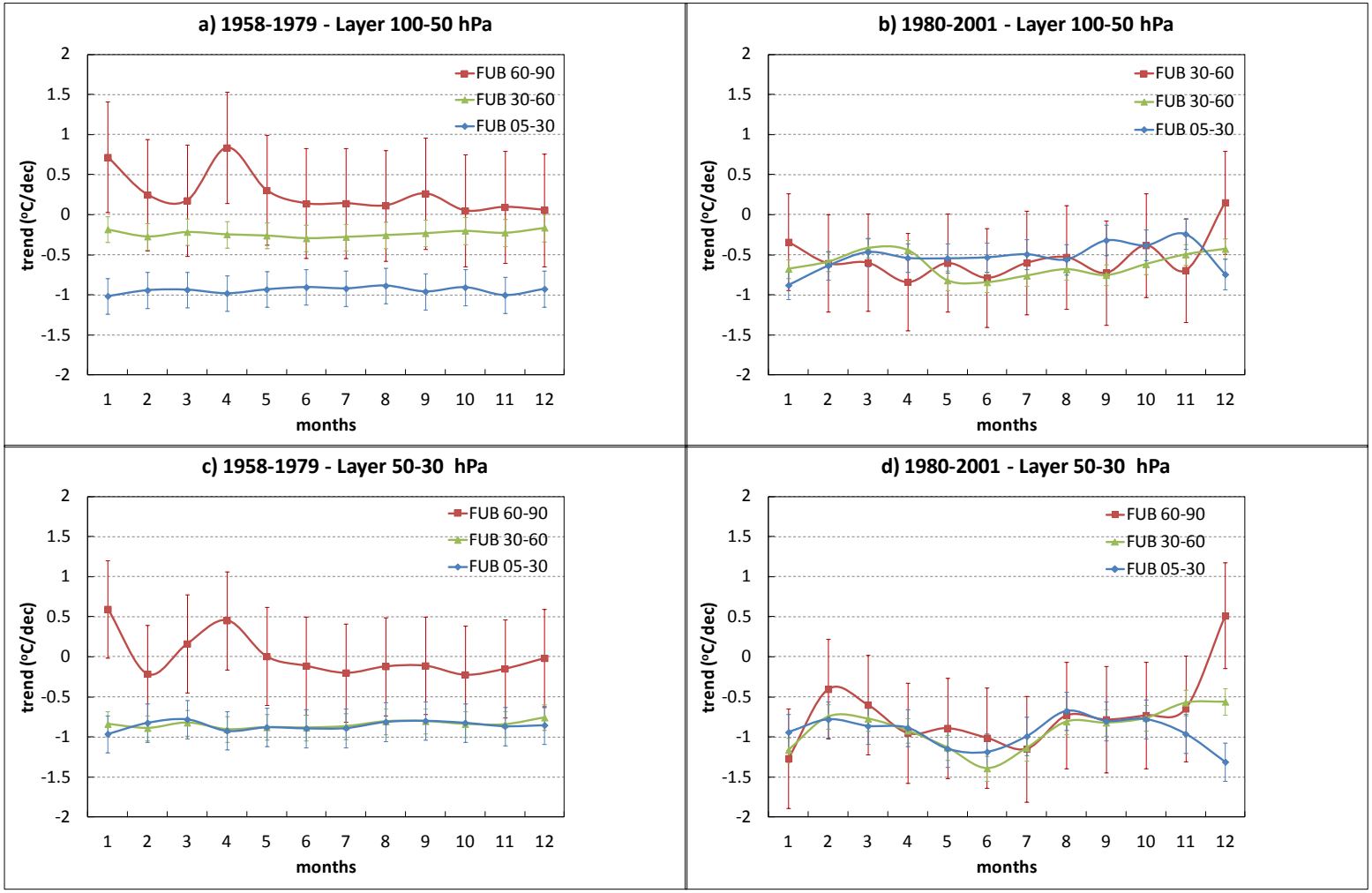

Figure 6: Layer mean temperature trends (°C/decade) for each month (x-axis) and layer (y-axis) based on WACCM model over the periods 1958-1979 and 1980-2005, respectively, for three latitudinal belts a) and b) for 5N-30N, c) and d) for 30N - 60N and e) and f) for 60N - 90N.

The layers are: Layer 1: 1000-925 hPa, Layer 2: 925-500 hPa, Layer 3: 500-300 hPa, Layer 4: 100-50 hPa, Layer 5: 50-30 hPa, and Layer 6: 30-10 hPa.

The shaded areas are non-statistically significant at 90% confidence level.

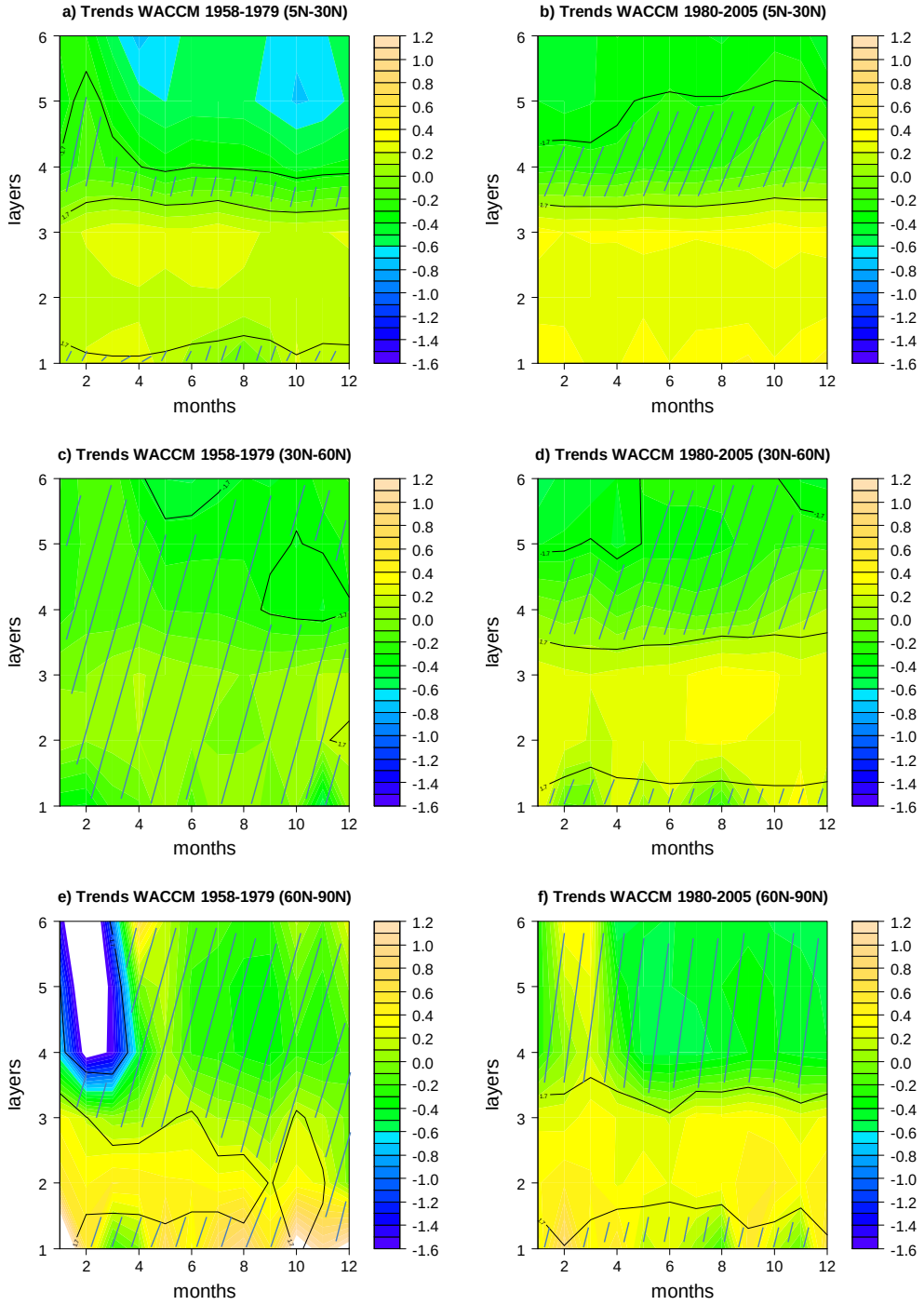

Figure 7: Correlation plots between tropopause pressure and layer mean temperature for each month (x-axis) and layer (y-axis) based on NCEP reanalysis (left panel) and WACCM model (right panel) over the common period 1958-2005 for the three latitudinal belts: 5N-30N (a and d), 30N - 60N (b and e) and 60N - 90N (c and f).

The layers are: Layer 1: 1000-925 hPa, Layer 2: 925-500 hPa, Layer 3: 500-300 hPa, Layer 4: 100-50 hPa, Layer 5: 50-30 hPa, and Layer 6: 30-10 hPa.

The contours indicate the statistically significant correlations at 95% significance level with $\rho>0.3$ or $\rho<-0.3$.

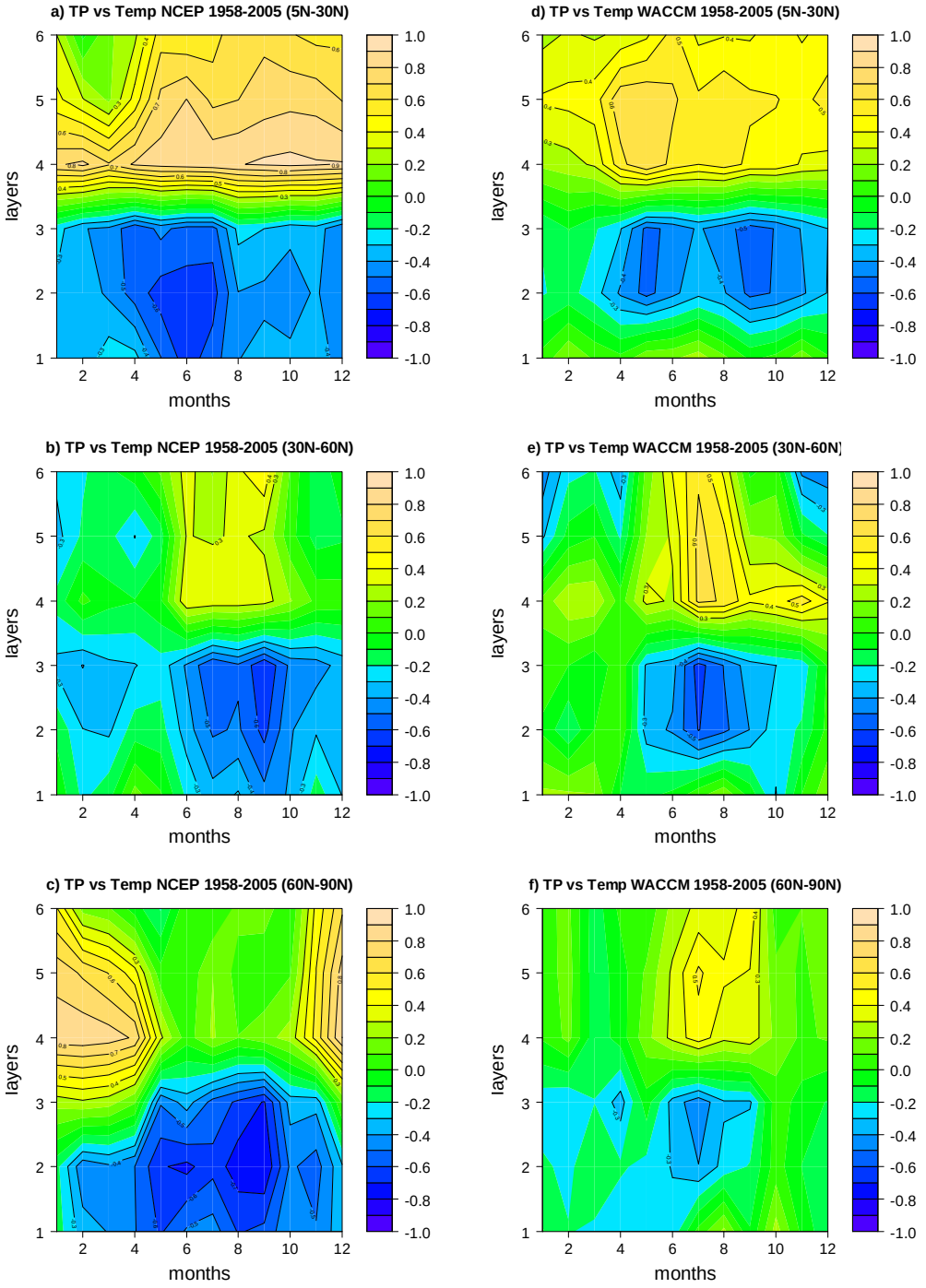

Conclusions

In conclusion, we provide additional evidence for an early greenhouse cooling signal of the lower stratosphere before the 1980s, which appears earlier than the tropospheric greenhouse warming signal. As a result, it may be that the stratosphere could have provided an early warning of human-produced climate change. In line with the theoretical expectations that equilibrium temperature in the stratosphere compared to the troposphere is more sensitive to anthropogenic GHGs and less sensitive to tropospheric water vapour, aerosols and clouds, it is tentatively proposed that the stratosphere is more suitable for the detection of man-made climate change signal. Our analysis also indicates that the relative contribution of the lower stratosphere versus the upper troposphere low frequency variability is important for understanding the added value of the long term tropopause variability related to human induced global warming.

We suggest that the maintenance and enrichment of the ground-based and satellite global networks for monitoring stratospheric temperatures and the tropopause region, which adds value in understanding the behaviour of the interface between the troposphere and stratosphere, are essential steps to unravel the issue of future human induced climate change signals.